



# Boosting Anion Transport Activity of Diamidocarbazoles by Electron Withdrawing Substituents

Krystyna Maslowska-Jarzyna, Maria L. Korczak and Michał J. Chmielewski\*

Faculty of Chemistry, Biological and Chemical Research Centre, University of Warsaw, Warsaw, Poland

Artificial chloride transporters have been intensely investigated in view of their potential medicinal applications. Recently, we have established 1,8-diamidocarbazoles as a versatile platform for the development of active chloride carriers. In the present contribution, we investigate the influence of various electron-withdrawing substituents in positions 3 and 6 of the carbazole core on the chloride transport activity of these anionophores. Using lucigenin assay and large unilamellar vesicles as models, the 3,6-dicyano- and 3,6-dinitro- substituted receptors were found to be highly active and perfectly deliverable chloride transporters, with  $EC_{50,270s}$  value as low as 22 nM for the  $Cl^-/NO_3^-$  exchange. Mechanistic studies revealed that diamidocarbazoles form 1:1 complexes with chloride in lipid bilayers and facilitate chloride/nitrate exchange by carrier mechanism. Furthermore, owing to its increased acidity, the 3,6-dinitro-substituted receptor acts as a pH-switchable transporter, with physiologically relevant apparent  $pK_a$  of 6.4.

**Keywords:** anion transport, chloride transport, pH-switchable transport, liposomes, LUVs, lucigenin, carbazole

## OPEN ACCESS

### Edited by:

Huaqiang Zeng,  
NanoBio Lab, A\*STAR, Singapore

### Reviewed by:

Zeyuan Dong,  
Jilin University, China  
Pengyang Xin,  
Henan Normal University, China

### \*Correspondence:

Michał J. Chmielewski  
mchmielewski@chem.uw.edu.pl

### Specialty section:

This article was submitted to  
Supramolecular Chemistry,  
a section of the journal  
Frontiers in Chemistry

**Received:** 01 April 2021

**Accepted:** 26 April 2021

**Published:** 20 May 2021

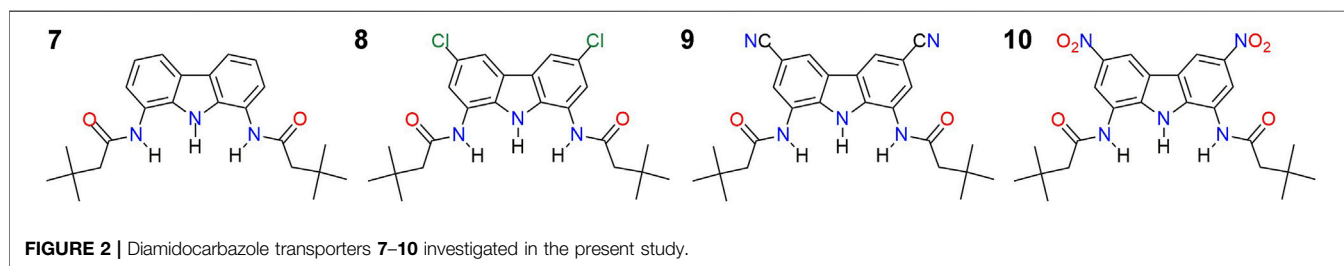
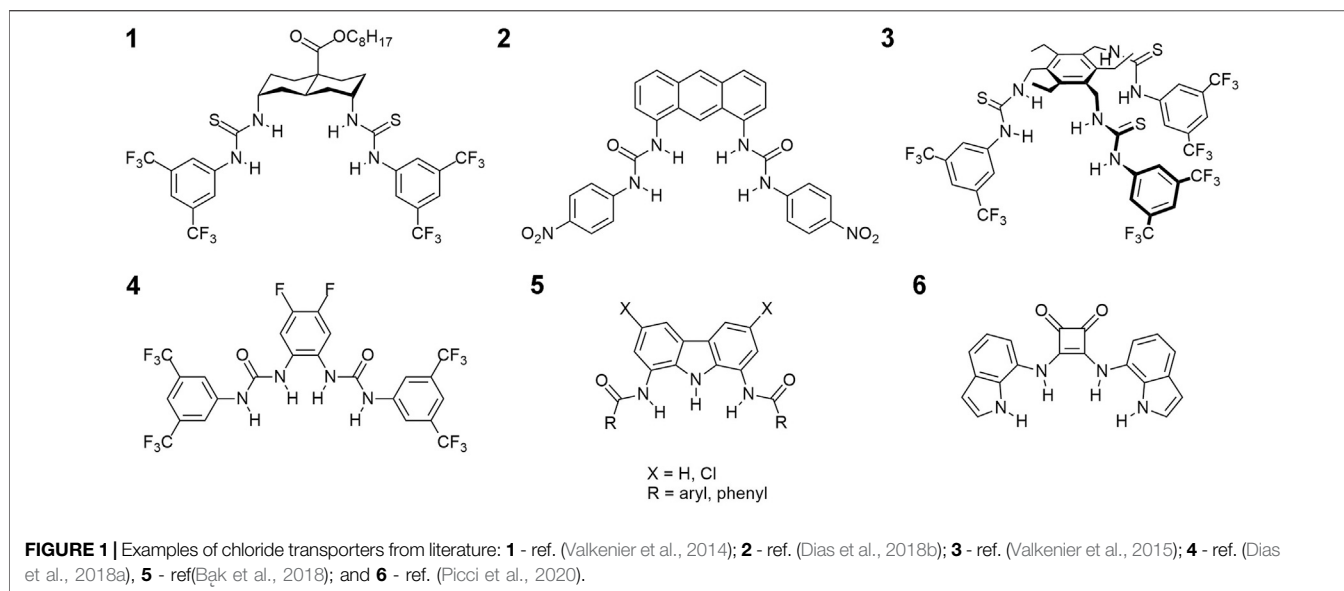
### Citation:

Maslowska-Jarzyna K, Korczak ML  
and Chmielewski MJ (2021) Boosting  
Anion Transport Activity of  
Diamidocarbazoles by Electron  
Withdrawing Substituents.  
Front. Chem. 9:690035.  
doi: 10.3389/fchem.2021.690035

## INTRODUCTION

Small molecules able to transport polar species through lipid bilayers are highly appealing for their potential biological activities (de Riccardis et al., 2013). This is because in living cells the concentration gradients of cations, anions and other polar solutes need to be precisely controlled and molecules that effectively perturb these gradients are very likely to influence biological functions (Sperelakis and Sperelakis, 2012). Indeed, many ionophores show antiviral, antibacterial and antifungal activities and some of them have been shown to act against insects, pests, and parasites (Kevin II et al., 2009). Significant research efforts have also been directed toward the development of novel antitumor, anti-inflammatory, antioxidant and neuroprotective ionophores (Ding and Lind, 2009; Kevin II et al., 2009; Kaushik et al., 2018).

Among other polar solutes, chloride transport is gaining increasing interest in recent years due to the growing appreciation of its physiological importance (Pusch, 2007). Chloride is the most abundant anion in the extracellular fluids, where its concentration typically exceeds 100 mM (Davis et al., 2007). In contrast, the intracellular  $Cl^-$  concentration is one order of magnitude lower and varies considerably between different cell types. The resulting chloride concentration gradients are important physiological parameters and in living cells they are precisely controlled by specialized proteins: pumps, channels and carriers. The transmembrane chloride transport they provide is important for  $CO_2$  excretion and pH regulation, neural signaling and maintaining cell volume (Pusch, 2007). Mutations in genes coding for these proteins are responsible for severe diseases, such as cystic fibrosis (Sheppard et al., 1993; Welsh and Smith, 1993), Bartter syndrome (Simon et al.,



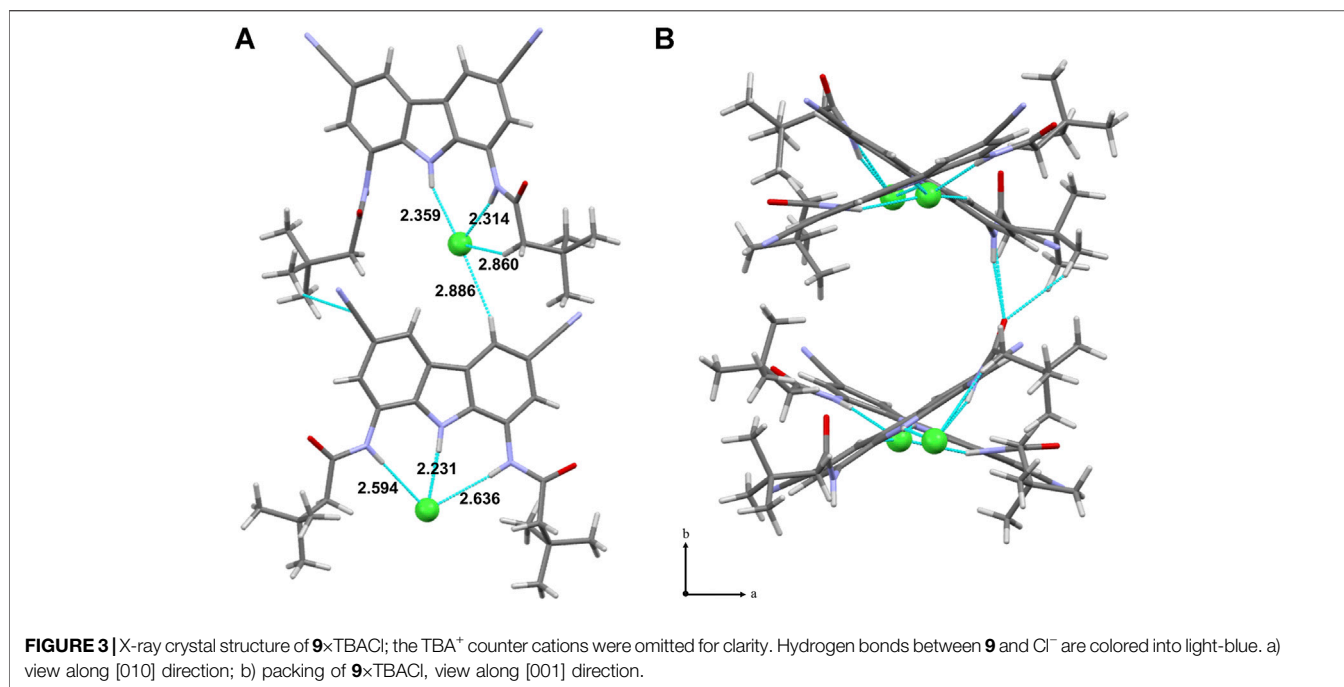
1996; Simon et al., 1997), and Dent's disease (Lloyd et al., 1996). One of the major driving forces behind the rapid development of artificial chloride transporters has been the idea that they might be used for treating these diseases (Gale et al., 2017; Davis et al., 2020). Apart from that, artificial chloride transporters have been shown to display also other interesting properties, such as anticancer and antibacterial activity (Elie et al., 2015; Saha et al., 2016).

Not surprisingly therefore, a flood of reports on artificial chloride transporters have been published in recent years (Valkenier et al., 2014; Dias et al., 2018b; Valkenier et al., 2015; Dias et al., 2018a; Bağ et al., 2018; Picci et al., 2020; Pomorski et al., 2021). Most of these reports concern uncharged, hydrogen bonding receptors with several hydrogen bond donors arranged in a convergent manner and a relatively lipophilic outer surface (for selected examples see **Figure 1**). Owing to these features the receptors preferentially dissolve in the lipid bilayer and effectively extract anions from water through the formation of supramolecular complexes which are sufficiently lipophilic to permeate the membrane. Ureas, thioureas and squaramides are among the most frequently used anion binding motifs in this type of molecules (Li et al., 2016), and perfluorinated residues are often attached to improve transport rates (Busschaert et al., 2011).

Recently, we have shown that simple and easy to make 1,8-diamidocarbazoles **5** (**Figure 1**) might also be developed into very active chloride carriers. Their transport activity can be easily modulated by varying the length and degree of branching of the amide side chains as well as by appropriate substitution of the carbazole core. Ion selective electrode (ISE) assay employing large unilamellar POPC vesicles (POPC LUVs) gave  $EC_{50}$  values down to 0.1  $\mu\text{M}$  for this initial set of carriers (Bağ et al., 2018).

To further improve the chloride transport activity of 1,8-diamidocarbazoles, we decided to introduce strongly electron withdrawing substituents in positions 3 and 6 of the carbazole core. Similar strategy has been successfully used to boost the activity of various ion carriers (Moore et al., 2013; Peng et al., 2016; Yu et al., 2018) and channels (Zeng et al., 2020). Recently, we have developed the synthesis of 3,6-dicyano and 3,6-dinitro substituted diamidocarbazoles **9** and **10** (**Figure 2**) and found that their chloride affinity is 6 and 7 times higher, respectively, in comparison to the unsubstituted **7**.<sup>1</sup> We found also that **9** and **10** are very prone to deprotonation. In this contribution, we study

<sup>1</sup>Masłowska-Jarżyna, K., Korczak, M. L., Wagner, J., and Chmielewski, M. J. (2021). Carbazole-based Colorimetric Anion Sensors. *Molecules*.submitted.



the chloride transport activity of the whole family of receptors **7–10** and investigate their mechanism of action, deliverability and pH dependent activity.

## RESULTS AND DISCUSSION

### The Synthesis of Model Transporters

Model receptors **7–10** were synthesized according to the previously published procedures (Bał and Chmielewski, 2014; Bał et al., 2018)<sup>1</sup>. In brief, chlorination of carbazole in positions 3 and 6 followed by nitration in positions 1 and 8 gives the key precursor – 3,6-dichloro-1,8-dinitrocarbazole **11**. This compound can be then either gently hydrogenated to yield 1,8-diamino-3,6-dichlorocarbazole, the substrate for the synthesis of **8**, or heated with hydrazine hydrate in the presence of Pd/C to give 1,8-diaminocarbazole, the acylation of which gives **7**. Similar strategy has been applied for the synthesis of **9**: bromination of carbazole and subsequent Pd-catalyzed Br to CN exchange gave 3,6-dicyanocarbazole (Weselinski et al., 2014), which can be cleanly nitrated in positions 1 and 8. Selective reduction of the 3,6-dicyano-1,8-dinitrocarbazole, followed by acylation, yields **9**. Finally, the synthesis of **10** starts from the commercially available 1,3,6,8-tetranitrocarbazole, which is selectively reduced in positions 1 and 8 and acylated to give **10**.

### X-Ray Crystallographic Studies

An X-ray crystal structure was obtained for the complex of **9** with TBACl. There are two crystallographically independent chloride complexes in the unit cell, both showing chloride anion bound inside the carbazole cleft, as expected. However, in one of the complexes the anion is held by all three NH moieties of the

receptor, whereas in the other—by only two (**Figure 3A**). This agrees with our previous presumptions that the chloride anion is too small to simultaneously form short hydrogen bonds with both amide groups of diamidocarbazoles. As a result, it either locates close to the middle of the binding cavity to form relatively long hydrogen bonds with both amides, or shifts to one side to maximize binding with only one amide. Both possibilities are nicely illustrated in the crystal structure of **9**×TBACl.

The aforementioned geometric mismatch between the binding cavity and the chloride anion is likely responsible for the relatively weak chloride affinity of diamidocarbazoles. As will be shown below, however, this rather weak binding is sufficient to ensure very fast chloride transport.

### Chloride Transport Studies

Previously, the anion transport properties of diamidocarbazoles were investigated using a standard ISE assay (Bał et al., 2018). In this method, a solution of a receptor in a water-miscible solvent, such as DMSO, is added to a suspension of LUVs in water. The typically lipophilic receptor then partially precipitates, and partially partitions between the lipid bilayer and aqueous phase. Although operationally simple and medically relevant, this assay is not particularly well suited for structure-activity relationship studies because the intrinsic activity trends might be blurred by poor deliverability of some receptors due to solubility issues. Therefore, in the present study, we chose a fluorescent assay, in which the receptor is pre-incorporated into the lipid membrane during the LUVs' preparation. In this method, the receptor-to-lipid ratio can be more precisely controlled.

On the other hand, even the most active transporters are not particularly attractive from medicinal chemistry point of view if they suffer from poor deliverability. This is likely to be the case for

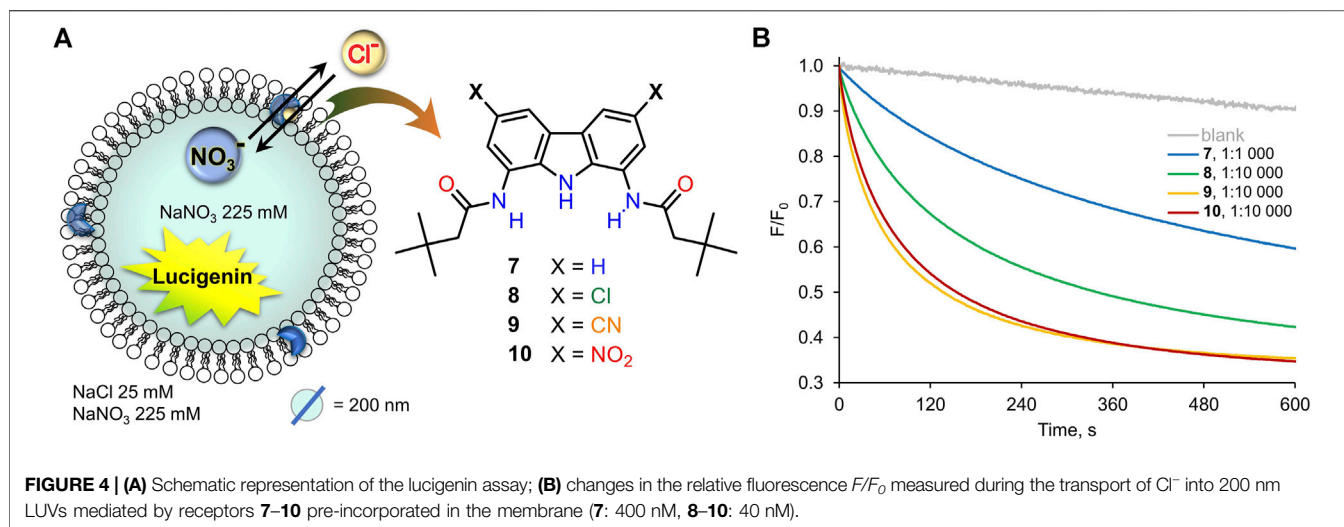


**TABLE 1 |** Binding and transport data for receptors **7–10**.

	$K_a$ [ $\text{M}^{-1}$ ] <sup>a)</sup>	$t_{1/2 \text{ pre}}$ [s] <sup>b)</sup>	$I_{\text{pre}}$ [ $\text{s}^{-1}$ ] <sup>c)</sup>	$I_{\text{post}}$ [ $\text{s}^{-1}$ ] <sup>c)</sup>	$\sigma_p$ <sup>d)</sup>	$D$ <sup>e)</sup>	$\text{clogP}$ <sup>f)</sup>
<b>7</b>	47.8	n.d. (648*)	n.d. (17*)	n.d.	0.00	n.d.	5.02
<b>8</b>	158.5	276	56	44	+0.23	0.79	5.85
<b>9</b>	309.0	140	126	146	+0.66	1.16	4.10
<b>10</b>	346.7	163	115	128	+0.78	1.11	4.61

n.d. = not determined; \* - parameters obtained for 1:1 000 transporter:lipid ratio. <sup>a)</sup> Obtained through  $^1\text{H}$  NMR titrations with TBACl in DMSO +0.5%  $\text{H}_2\text{O}$  at 298 K (Bak et al., 2018;)<sup>1</sup>.

<sup>b)</sup> Half-life times  $t_{1/2}$  obtained from fitting of  $F_0/F$  (0–600 s) traces to a single exponential function for pre-incorporated **7–10** at transporter-to-lipid ratio 1:10,000. <sup>c)</sup> Initial rate  $I$  obtained from fitting of  $F_0/F$  (0–600 s) traces to a double exponential function for pre-incorporated ( $I_{\text{pre}}$ ) or post-incorporated ( $I_{\text{post}}$ ) **7–10**; transporter:lipid = 1:10,000. <sup>d)</sup> Hammett parameters for substituents in positions 3 and 6. <sup>e)</sup> Deliverability  $D$  calculated as the ratio of initial transport rates derived from experiments with post- and pre-incorporated transporter, transporter-to-lipid ratio 1:10,000. <sup>f)</sup> Calculated  $\text{logP}$  values predicted using ALOGPS 2.1 software;  $p$  is the partition coefficient of the receptor between *n*-octanol and water.

diamidocarbazoles, because they are very poorly soluble in water and in most organic solvents (except for aprotic dipolar solvents such as DMSO and DMF). To address this issue, we directly compared the activity of pre-incorporated and post-incorporated transporters.

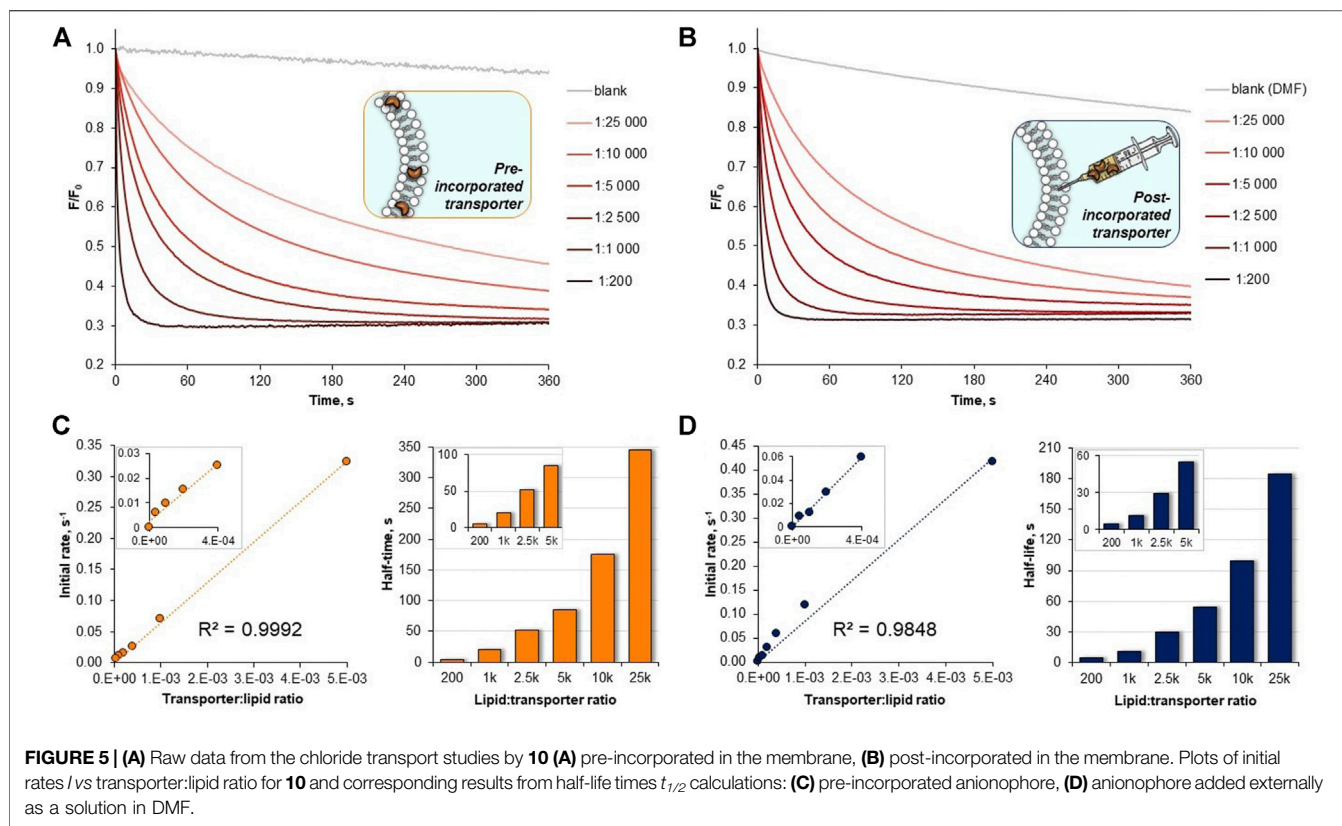
Thus, the chloride transport by **7–10** was initially studied using the very well-known lucigenin assay for  $\text{Cl}^-/\text{NO}_3^-$  exchange, schematically shown in **Figure 4** (Valkenier et al., 2014). LUVs (mean diameter 200 nm) were grown from a lipid mixture composed of POPC and cholesterol (in 7:3 ratio) with the appropriate transporter at a given concentration, in the presence of halide-sensitive dye, lucigenin (0.8 mM), and  $\text{NaNO}_3$  (250 mM). Unencapsulated lucigenin was separated from vesicles by gel filtration. Such liposomes were then suspended in aqueous  $\text{NaNO}_3$  (225 mM), diluted to 0.4 mM and transferred to a spectrofluorometer. The experiment was commenced by the addition of  $\text{NaCl}$  (1M in 225 mM  $\text{NaNO}_3$ ) to a final concentration of 25 mM. The addition of  $\text{NaCl}$  resulted in an immediate drop of fluorescence intensity due to quenching of the residual unencapsulated lucigenin, followed by a gradual decrease of fluorescence due to the transport-mediated quenching of the internal lucigenin by chlorides (**Figure 4A**).

All the carbazole-based receptors **7–10** were found to be active chloride transporters under these conditions (**Figure 4B**).

However, the electron-deficient **8–10** promoted much faster transport than the unsubstituted **7** (note that in **Figure 4B** the concentrations of **8–10** are 10 times lower than **7**). The 1:10,000 receptor-to-lipid ratio corresponds to just 0.01 mol% concentration of the receptor in the bilayer and 0.04  $\mu\text{M}$  in the whole vesicle suspension. Even when present in so tiny amounts, the most active carriers **9** and **10** almost completely equilibrate chloride concentrations on both sides of the membrane in 10 min.

The transport rates were quantified by fitting the inverse of the normalized fluorescence traces  $F_0/F$  to a single exponential function to obtain approximate half-lives  $t_{1/2}$  and to a double exponential function to obtain initial rates  $I$ . Results are summarized in **Table 1**.

The most noticeable result is a huge, more than tenfold, increase in activity upon introduction of moderately electron withdrawing chlorine substituents in positions 3 and 6 of the carbazole core. This effect has already been noted in our previous study using ISE assay, but the results presented here prove that it is related to the intrinsic activities of **7** and **8**. Receptor **8** has 3 times higher chloride affinity than **7** and also higher  $\text{clogP}$  value, so we presume that the combined effect of these two changes is responsible for such a strong impact on ionophoric activity.



Further increase in electron withdrawing strength from Cl to CN increases the chloride transport rate more than twofold, in line with the *ca.* twofold increase in anion affinity. It is well known, however, that many other factors have significant impact on the observed transport rates, so this correlation might be a coincidence. In fact, the CN-substituted receptor **9** is also much less lipophilic than **8**, with  $\text{clogP} = 4.10$  vs. 5.85 for **8**.

Finally, the most electron withdrawing  $\text{NO}_2$  substituents slightly decrease the transport activity of **10**, despite increased chloride affinity and higher lipophilicity in comparison to **9**. As will be shown below, this is probably due to partial deprotonation of **10** under these conditions.

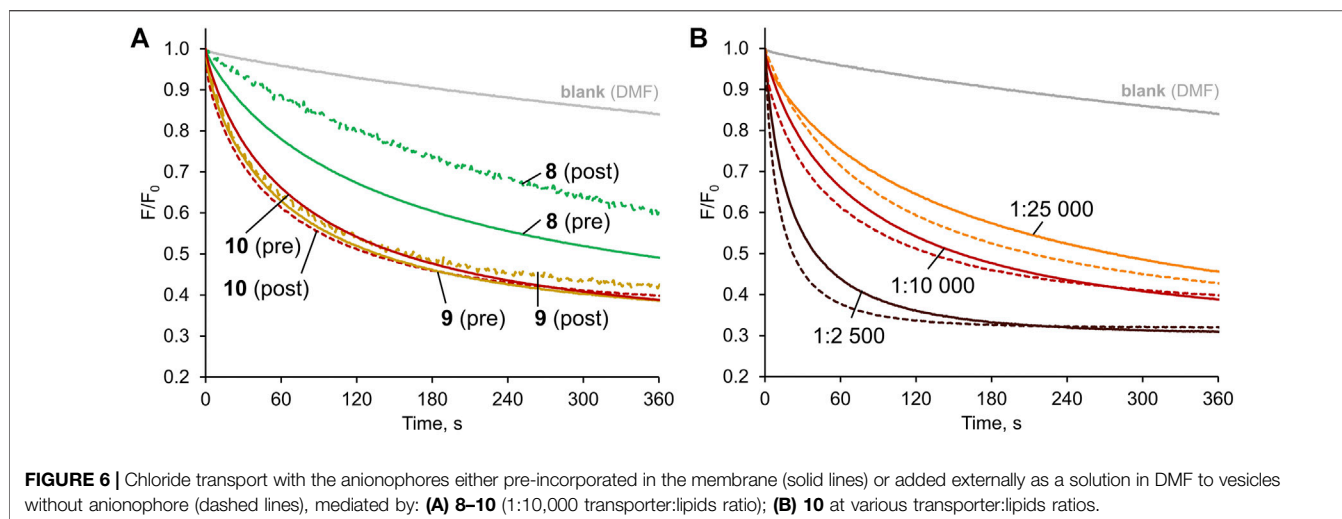
Dose-activity studies were performed for **10** to allow for Hill analysis and calculation of  $\text{EC}_{50,270\text{s}}$  value (Figure 5A). In our assay, this value refers to the concentration of pre-incorporated transporter required to rise the intravesicular chloride concentration to 50% of the initial gradient during 270 s. Using  $F_0/F$  as a measure of chloride concentration inside the vesicles, we plotted the values recorded at 270 s against the concentration of transporter **10** in the membrane and fitted the data with the Hill equation (Supplementary Figure S36). Using this procedure,  $\text{EC}_{50,270\text{s}}$  of 22.4 nM (0.0056 mol% with respect to lipids) was obtained. Although it is difficult to compare literature values obtained under different conditions and using different assays, this level of activity certainly ranks **10** among the most active artificial transporters known to date.

Hill analysis also allows for the Hill coefficient to be determined, which indicates the number of receptor molecules

in the active complex. The calculated value of  $1.08 \pm 0.07$  indicates that **10** acts as a mobile carrier and not as a channel. This is in agreement with the linear correlation between the initial transport rates and the transporter concentration, presented in Figure 5C.

To shed more light on the mechanism of anion transport by **7–10**, additional control experiments were performed in which the relatively lipophilic  $\text{NO}_3^-$  anions were replaced by highly hydrophilic  $\text{SO}_4^{2-}$  in both internal and external solutions (Grauwels et al., 2019). No significant anion transport was detected under these conditions (ESI, Supplementary Figure S4), which means that the  $\text{Cl}^-/\text{NO}_3^-$  exchange is the most likely mechanism for the transport activity displayed by **7–10**. Similar results were previously obtained for other diamidocarbazoles and di(thioamido)carbazoles (Bağ et al., 2018; Pomorski et al., 2021).

Having established diamidocarbazoles **8–10** as very active chloride transporters, we next sought to investigate how readily they could be delivered into lipid membranes by post-assembly addition. As mentioned before, this is an important aspect of practical effectiveness and sometimes even the most active synthetic transporters are unable to pass this test satisfactorily (Valkenier et al., 2014; Mora et al., 2016). To investigate deliverability, LUVs were prepared in a manner analogous to that previously described, except that no anionophore was added to the initial lipid mixture. Instead, 5  $\mu\text{L}$  of concentrated solution of receptor in DMF (Dias et al., 2018b) was added to the rapidly stirred suspension of preformed



vesicles. After 3 min of stirring, 1M NaCl was added and the decay in fluorescence was measured as before (Figure 6).

Visually, the traces for pre-incorporated and post-incorporated **9** and **10** are close to each other, meaning that the deliverability of these receptors is very good. Much more significant difference was observed between the respective traces for **8**, while **7** was not investigated due to the greatly inferior activity.

To quantify the effect, the deliverability factor  $D$  was calculated for **8–10** by dividing the initial rate of transport for post-incorporated receptor by the value obtained for pre-incorporated anionophore. In theory, for perfectly deliverable transporters,  $D$  should be equal to 1. However, the actual concentration of lipids is always lower than the nominal value due to losses during vesicle preparation, and therefore in experiments with post-incorporated receptors the real transporter-to-lipid ratio is always higher than intended (Bağ et al., 2018). As a result,  $D$  is sometimes higher than 1 and this was indeed observed for **9** and **10**. The same effect can be observed by comparing the  $F/F_0$  traces for post- and pre-incorporated **10** at various receptor-to-lipid ratios—the post-incorporated ionophore consistently shows higher apparent activity (Figure 6B). On the contrary, however, **8** displayed inferior activity when added externally, indicating that this receptor is not perfectly deliverable ( $D = 0.79$ ). Even in this least favourable case, however, the deliverability issue is not so severe as to rule out potential applications of this anionophore.

## pH-Dependent Transport Studies

pH-switchable anionophores are particularly attractive for their potential medical applications. Such compounds may be used to specifically target chloride transport in acidic cells and organelles, and to couple chloride transport with proton gradients. Since cancer cells are generally associated with lower pH values than healthy cells, it would be very beneficial if synthetic transporters could effectively switch ON in acidic environment and OFF at neutral pH. To date, however, there are only few reports on pH-dependent transporters (Busschaert et al., 2014; Elmes et al., 2015;

Howe et al., 2016; Saha et al., 2019; Wang et al., 2021) and highly active carriers that possess very specific pH-regulated ON/OFF function are still unavailable.

The 3,6-dinitro substituted diamidocarbazole **10** is significantly more acidic than other diamidocarbazoles, so we were curious if it may function as pH-switchable carrier. To address this question experimentally, we decided to use the lucigenin method. Lucigenin fluorescence is not significantly affected by pH up to 11 (Bağ et al., 2021), so it seemed to be well suited for this purpose. To the best of our knowledge, however, related studies of pH-dependent chloride transport using lucigenin assay have not been reported in the literature, despite its ease and availability.

The results of our pH-dependent transport experiments are shown in Figure 7. Quantification of the transport rates was accomplished as before, by fitting each  $F_0/F$  curve (0–600 s) to a double exponential decay function in order to determine initial rates  $I$ . As expected, the transport activity of **10** is indeed the highest at acidic pH, and drops significantly at pH close to neutral (Figure 7). The particularly striking decrease in activity was observed between pH 6.1 and 6.7, where this small pH change reduces transport rate ca. 2-fold. The plot of the initial transport rates vs. pH was used to calculate the apparent  $pK_a$  of **10** in the membrane environment, according to the method developed by Gale and co-workers (see ESI for details) (Busschaert et al., 2014). The obtained value of apparent  $pK_a = 6.4$  is very close to physiological pH.

## CONCLUSION

Simple diamidocarbazoles with highly electron withdrawing nitro- and cyano-substituents in the carbazole core have been established as extremely active and perfectly deliverable chloride transporters in large unilamellar vesicles. Compound **10** gave a very low  $EC_{50, 270s}$  value of 22.4 nM in the chloride/nitrate assay, which is particularly impressive considering its simple structure and easy availability. Mechanistic studies revealed that diamidocarbazoles act as chloride/nitrate exchangers and form

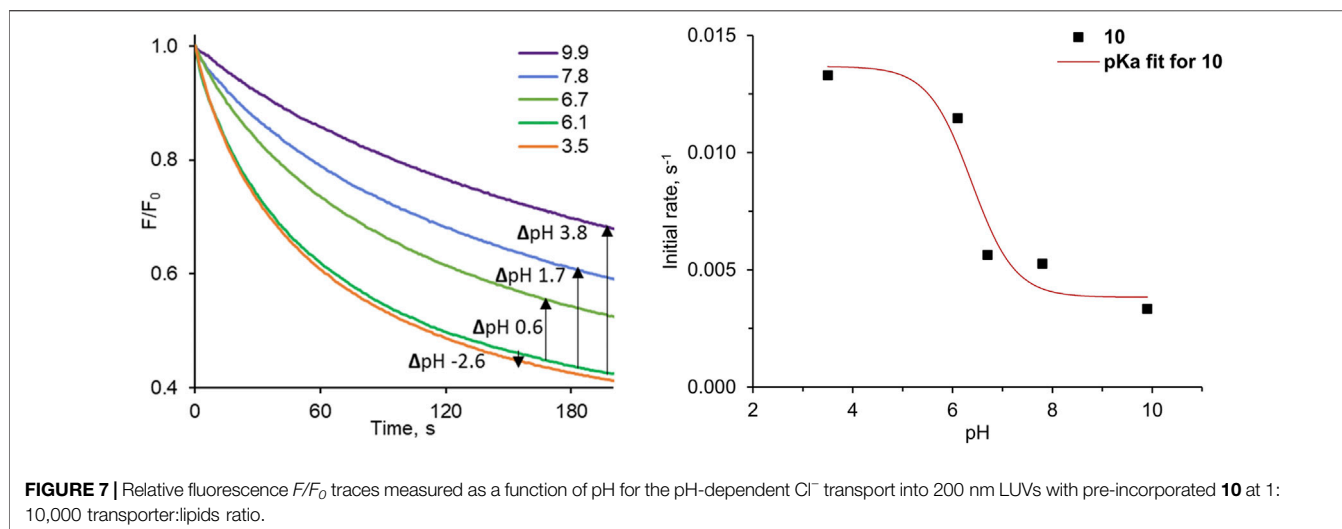


**FIGURE 7** | Relative fluorescence  $F/F_0$  traces measured as a function of pH for the pH-dependent  $Cl^-$  transport into 200 nm LUVs with pre-incorporated **10** at 1:10,000 transporter:lipids ratio.

1:1 complexes with chloride while carrying it through lipid bilayers. The 3,6-dinitro substituted receptor **10** is much more acidic than other diamidocarbazoles and hence its activity is significantly dependent on pH. The receptor is most active in mildly acidic medium and loses much of its activity at pH close to physiological. Taken together, all these findings make **10** a very promising lead compound for further development of chloride transporters for medicinal applications.

## MATERIALS AND METHODS

### Abbreviations

ISE: ion-selective electrode  
 LUV: large unilamellar vesicle  
 POPC: 1-palmitoyl-2-oleoyl-*sn*-glycero-3-phosphocholine;  
 DMSO: dimethyl sulfoxide.

### Materials

All solvents and reagents were commercially available and used as received unless otherwise stated.

Water was taken from Milli-Q purification system.

### Chempur

Methanol (116219904, >99.8%).

### GE Healthcare

Sephadex G-50 superfine (17004101).

### Sigma-Aldrich

Aluminum oxide (199443, activated, basic), *N,N'*-dimethyl-9,9'-biacridinium dinitrate (lucigenin, M8010), chloroform (for HPLC, stab. with amylene, 34,854-1L-M,  $\geq 99.8\%$ ), cholesterol (C8667, >99.5%), nitric acid (84,378, puriss. p. a., 65–67%), 2-oleoyl-1-palmitoyl-*sn*-glycero-3-phosphocholine (POPC, 850457C, >99%, Avanti PC and LPC), sodium hydroxide solution (2 N, Titripur, 1091361000), sodium nitrate (221341,  $\geq 99.0\%$ ).

### VWR

Dimethylformamide (DMF, for HPLC, 83635320, >99.90%).

## Instruments and Methods

### Weighing

Mettler Toledo Excellence XA105DU analytical balance was used for weighing all the samples.

### Fluorescence spectroscopy

Fluorescence spectra were acquired using Hitachi F-7000 spectrophotometer equipped with Peltier temperature controller. Screw-capped SUPRASIL quartz fluorescence cuvettes (optical path length: 10 mm) were used.

### Vortexing

IKA VORTEX 4 basic, model V 4 B S000 was used for vortexing during LUVs preparation.

### Extrusion

AVESTIN LiposoFast-Basic with polycarbonate membranes with pore sizes of 200 nm was used for extrusion during LUVs preparation.

## Synthesis of Receptors 7–10

Transporters **7–10** were obtained as described previously. (Bąk et al., 2018; Bąk and Chmielewski, 2014)<sup>1</sup>.

## General Procedure for Measuring the Transport of Chlorides in LUVs Using Pre-incorporated Receptors

The general procedure is a slightly modified version of the chloride transport protocol published previously (Valkenier et al., 2014). In a 5 ml round bottom flask the mixture of 420  $\mu L$  of 10 mM POPC and 180  $\mu L$  of 10 mM cholesterol (7:3 M ratio) was prepared in chloroform which was previously deacidified by passing through a pad of activated basic alumina.

10  $\mu\text{L}$  of a solution of an appropriate anionophore 7–10 (0.024 mM, 0.06 mM, 0.24 mM, or 3 mM in  $\text{CHCl}_3\text{:MeOH}$  1:1 v/v) were added to the lipids solution at 0–0.5 mol% ratio relative to the total amount of lipids. Neither the receptor solution nor pure  $\text{CHCl}_3\text{:MeOH}$  1:1 v/v were added when the blank was measured (0 mol%). The organic solvents were evaporated on a rotary evaporator and the residue was dried under high vacuum for 1 h. The lipid film was hydrated with 0.500 ml of aqueous solution containing lucigenin (0.8 mM) and  $\text{NaNO}_3$  (225 mM) or  $\text{Na}_2\text{SO}_4$  (112 mM), sonicated for 30 s and vortexed for 1 h resulting in vesicle formation. The multilamellar vesicles were broken down into unilamellar vesicles by 10 freeze-thawing cycles, diluted to 1 ml by the addition of  $\text{NaNO}_3$  (225 mM) or  $\text{Na}_2\text{SO}_4$  (112 mM), and extruded 29 times through a polycarbonate membrane (200 nm pore size) to give homogeneous large unilamellar vesicles. Unencapsulated lucigenin was removed by passing the mixture through a column with Sephadex 50G (ca. 2 g, superfine) using an aqueous  $\text{NaNO}_3$  (225 mM) or  $\text{Na}_2\text{SO}_4$  (112 mM) as eluent. The collected vesicles were diluted with  $\text{NaNO}_3$  (225 mM) or  $\text{Na}_2\text{SO}_4$  (112 mM) to 15 ml (lipid concentration  $\approx 0.4$  mM). 3 ml of the vesicle suspension was placed in a quartz cuvette with a small stirring bar and its fluorescence was measured as a function of time (excitation: 455 nm, emission: 505 nm). Aqueous  $\text{NaCl}$  (75  $\mu\text{L}$ , 1.0 M in 225 mM  $\text{NaNO}_3$  or 112 mM  $\text{Na}_2\text{SO}_4$ , to give an overall external chloride concentration of 25 mM) was added 30 s after the start of fluorescence measurement. The fluorescence intensity was measured for 15 min. For each run the initial plateau (before the addition of chloride) and the vertical drop (the first 0.5–2 s after chloride addition) due to quenching of residual external lucigenin were removed. Next, the data were normalized: all fluorescence values ( $F$ ) were divided by the maximum fluorescence value ( $F_0$ ).

### General Procedure for Measuring the Transport of Chlorides in LUVs Induced by Externally Added Transporter

LUVs were prepared in the same manner as described in Section 4.5, except that the anionophore was not added to the initial lipid mixture. After size exclusion chromatography, the collected vesicles were diluted with aqueous  $\text{NaNO}_3$  (225 mM) to 15 ml (lipid concentration  $\approx 0.4$  mM) and 3 ml of this was transferred to a cuvette with a small stirring bar. Solutions of anionophores 7–10 were prepared in DMF (Dias et al., 2018b) at several concentrations: 1200  $\mu\text{M}$ , 240  $\mu\text{M}$ , 96  $\mu\text{M}$ , 48  $\mu\text{M}$ , 24  $\mu\text{M}$ , 9.6  $\mu\text{M}$ , 4.8  $\mu\text{M}$ , 2.4  $\mu\text{M}$ , 0.96  $\mu\text{M}$ , 0.48  $\mu\text{M}$ . Anionophore solution (5  $\mu\text{L}$ ) was then added to the vesicle suspension in the cuvette, employing a 25  $\mu\text{L}$  syringe with rapid plunger action and with the tip of the syringe needle positioned just above the stir bar. Assuming the lipid concentration of 0.4 mM, this would give a transporter to lipid ratio of 1:200, 1:1 000, 1:2 500, 1:5 000, 1:10,000, 1:25,000, 1:50,000, 1:100,000, 1:250,000 or 1:500,000 respectively. Aqueous  $\text{NaCl}$  (75  $\mu\text{L}$ , 1.0 M in 225 mM  $\text{NaNO}_3$ , to give an overall external chloride concentration of 25 mM) was added 3 min after the anionophore addition and 30 s after the

start of fluorescence measurements. The fluorescence intensity was measured for 15 min (excitation: 455 nm, emission: 505 nm). Pure DMF (5  $\mu\text{L}$ ) was added followed by the addition of aqueous  $\text{NaCl}$  (75  $\mu\text{L}$ , 1.0 M in 225 mM  $\text{NaNO}_3$ ) to measure blank. The plateau (before addition of anions) and the vertical drop (the first 0.5–2 s after the addition of anions) due to quenching of residual external lucigenin were removed. The data are normalized: all fluorescence values ( $F$ ) were divided by the fluorescence value measured before the addition of anion ( $F_0$ ).

### Investigation of pH-dependent Chloride Transport

LUVs were prepared in the same manner as described in Section 4.5, except that transporter 10 (0.0015 M in  $\text{CHCl}_3\text{:MeOH}$  1:1 v/v) was diluted to a concentration of 60  $\mu\text{M}$  and added to the lipids solution at 0.1 mol% (1:10,000) ratio relative to the total amount of lipids. After size exclusion chromatography, the collected vesicles were diluted with aqueous  $\text{NaNO}_3$  (225 mM) to 15 ml (lipid concentration  $\approx 0.4$  mM) and 3 ml of this was transferred to a cuvette with a small stirring bar. Calculated amounts of diluted solutions of  $\text{NaOH}$  or  $\text{HNO}_3$  were added to the liposomes suspension to achieve an appropriate pH. Additionally, final pH in each cuvette was measured using a pH-meter. Aqueous  $\text{NaCl}$  (75  $\mu\text{L}$ , 1.0 M in 225 mM  $\text{NaNO}_3$ , to give an overall external chloride concentration of 25 mM  $\text{Cl}^-$ ) was added 30 s after the start of fluorescence measurements. For each run the initial plateau (before the addition of chloride) and the vertical drop (the first 0.5–2 s after chloride addition) due to quenching of residual external lucigenin were removed. The data are normalized: all fluorescence values ( $F$ ) were divided by the maximum fluorescence value ( $F_0$ ).

### Quantification of Transport Rates

As described in previous publications (Elie et al., 2015), the inverse of the normalized fluorescence trace ( $F_0/F$ ) is directly proportional to the concentration of chloride inside the vesicles (according to the Stern-Volmer equation). Thus  $F_0/F$  was used in the quantification of transport rates.

Half-life time,  $t_{1/2}$ : determined by fitting the  $F_0/F$  curve (0–600 s) to a single exponential decay function:

$$F_0/F = y - a \cdot \exp(-bt),$$

Obtaining a value for the fit parameter  $b$  allows for the half-life  $t_{1/2}$  to be calculated:

$$t_{1/2} = \ln(2)/b,$$

Initial rate,  $I$ : determined by fitting of the  $F_0/F$  curve (0–600 s) to a double exponential decay function:

$$F_0/F = y - a \cdot \exp(-bt) - c \cdot \exp(-dt),$$

Differentiating at  $t = 0$  allows for the initial rate  $I$  to be calculated:

$$I = (a \cdot b) + (c \cdot d),$$

Using  $F_0/F$  values at 270 s as a measure of chloride concentration inside the vesicles at that time, these values were plotted against the

corresponding concentration of transporter used for different loadings of transporter. The data were fitted with the Hill equation in Origin 2021 (**Supplementary Figures S36–S37**).

## X-Ray Measurement

For crystallizations of  $9 \times \text{Cl}^-$  complex, dichloroethane solution of **9** with excess of TBACl salt was mixed with pentane, placed into vials and NMR tubes, capped and left standing. Red crystalline material precipitated in NMR tube. Suitable crystal was chosen for the X-ray measurement.

Diffraction data were collected on the Agilent Technologies SuperNova Dual Source with the MoK $\alpha$  radiation ( $\lambda = 0.71073 \text{ \AA}$ ). The lattice parameters were obtained by least-squares fit to the optimized setting angles of the reflections collected by using the CrysAlis CCD software (Oxford Diffraction, 2008). Data were reduced using the CrysAlis RED program (Oxford Diffraction, 2008). The Gaussian numerical absorption correction using a multifaceted crystal model implemented in SCALE3 ABSPACK scaling algorithm, was applied (Oxford Diffraction, 2008). Using Olex2 (Dolomanov et al., 2009), the structure was solved with the ShelXT (Sheldrick, 2015b) structure solution program using Intrinsic Phasing and refined with the ShelXL (Sheldrick, 2015a) refinement package using Least Squares minimization. All H-atoms were positioned geometrically. The crystallographic data are summarized in **Supplementary Table S1**. The values of bond lengths and valence angles are given in **Supplementary Tables S2–S3**.

Data Availability Statement: Crystallographic data for the structure in this paper have been deposited with the Cambridge Crystallographic Data Center as supplementary publication number CCDC 2074654. Copies of the data can be obtained, free of charge, on application to CCDC [e-mail: deposit@ccdc.cam.ac.uk, website: www.ccdc.cam.ac.uk].

## DATA AVAILABILITY STATEMENT

The datasets presented in this study can be found in online repositories. The names of the repository/repositories and

accession number(s) can be found in the article/**Supplementary Material**.

## AUTHOR CONTRIBUTIONS

KM-J: conceptualization, methodology, data analysis, visualization, writing and editing of the manuscript. MK: synthesis of receptors, methodology, data analysis. MC: conceptualization, funding acquisition, supervision, data analysis, writing, and editing of the manuscript. All authors contributed to the article and approved the submitted version.

## FUNDING

This work was supported by the National Science Center, Poland (OPUS grant 2018/31/B/ST5/02085 to MC). This study was carried out at the Biological and Chemical Research Center, University of Warsaw, established within a project co-financed by the European Union through the European Regional Development Fund under the Operational Programme Innovative Economy 2007–2013.

## ACKNOWLEDGMENTS

We thank Dr. Szymon Sutuła from the Core Facility for Crystallography and Biophysics for the excellent crystallographic service he provides.

## SUPPLEMENTARY MATERIAL

The Supplementary Material for this article can be found online at: <https://www.frontiersin.org/articles/10.3389/fchem.2021.690035/full#supplementary-material>

## REFERENCES

- Bąk, K. M., Chabuda, K., Montes, H., Quesada, R., and Chmielewski, M. J. (2018). 1,8-Diamidocarbazoles: an Easily Tuneable Family of Fluorescent Anion Sensors and Transporters. *Org. Biomol. Chem.* 16, 5188–5196. doi:10.1039/C8OB01031E
- Bąk, K. M., and Chmielewski, M. J. (2014). Sulfate Templated Assembly of Neutral Receptors in Aqueous DMSO – Orthogonal versus Biplane Structures. *Chem. Commun.* 50, 1305–1308. doi:10.1039/C3CC48463G
- Bąk, K. M., van Kolck, B., Masłowska-Jarżyna, K., Papadopoulou, P., Kros, A., and Chmielewski, M. J. (2021). Oxyanion Transport Across Lipid Bilayers: Direct Measurements in Large and Giant Unilamellar Vesicles. *Chem. Commun.* 56, 4910–4913. doi:10.1039/C9CC09888G
- Busschaert, N., Elmes, R. B. P., Czech, D. D., Wu, X., Kirby, I. L., Peck, E. M., et al. (2014). Thiosquaramides: pH Switchable Anion Transporters. *Chem. Sci.* 5, 3617–3626. doi:10.1039/C4SC01629G
- Busschaert, N., Wenzel, M., Light, M. E., Iglesias-Hernández, P., Pérez-Tomás, R., and Gale, P. A. (2011). Structure-Activity Relationships in Tripodal Transmembrane Anion Transporters: The Effect of Fluorination. *J. Am. Chem. Soc.* 133, 14136–14148. doi:10.1021/ja205884y
- Davis, J. T., Gale, P. A., and Quesada, R. (2020). Advances in Anion Transport and Supramolecular Medicinal Chemistry. *Chem. Soc. Rev.* 49, 6056–6086. doi:10.1039/C9CS00662A
- Davis, P., Sheppard, D. N., and Smith, B. D. (2007). Development of Synthetic Membrane Transporters for Anions. *Chem. Soc. Rev.* 36, 348–357. doi:10.1039/B512651G
- de Riccardis, F., Izzo, I., Montesarchio, D., and Tecilla, P. (2013). Ion Transport through Lipid Bilayers by Synthetic Ionophores: Modulation of Activity and Selectivity. *Acc. Chem. Res.* 46, 2781–2790. doi:10.1021/ar4000136
- Dias, C. M., Li, H., Valkenier, H., Karagiannidis, L. E., Gale, P. A., Sheppard, D. N., et al. (2018a). Anion Transport by Ortho-Phenylene Bis-Ureas across Cell and Vesicle Membranes. *Org. Biomol. Chem.* 16, 1083–1087. doi:10.1039/c7ob02787g
- Dias, C. M., Valkenier, H., and Davis, A. P. (2018b). Anthracene Bisureas as Powerful and Accessible Anion Carriers. *Chem. Eur. J.* 24, 6262–6268. doi:10.1002/chem.201800508
- Ding, W.-Q., and Lind, S. E. (2009). Metal Ionophores – an Emerging Class of Anticancer Drugs. *IUBMB Life.* 61, 1013–1018. doi:10.1002/iub.253

- Dolomanov, O. V., Bourhis, L. J., Gildea, R. J., Howard, J. A. K., and Puschmann, H. (2009). OLEX2: A Complete Structure Solution, Refinement and Analysis Program. *J. Appl. Cryst.* 42, 339–341. doi:10.1107/S0021889808042726
- Elmes, R. B. P., Busschaert, N., Czech, D. D., Gale, P. A., and Jolliffe, K. A. (2015). pH Switchable Anion Transport by an Oxothiosquaramide. *Chem. Commun.* 51, 10107–10110. doi:10.1039/c5cc03625a
- Elie, R., David, G., and Schmitzer, A. R. (2015). Strong Antibacterial Properties of Anion Transporters: A Result of Depolarization and Weakening of the Bacterial Membrane. *J. Med. Chem.* 58, 2358–2366. doi:10.1021/jm501979f
- Gale, P. A., Davis, J. T., and Quesada, R. (2017). Anion Transport and Supramolecular Medicinal Chemistry. *Chem. Soc. Rev.* 46, 2497–2519. doi:10.1039/C7CS00159B
- Grauwels, G., Valkenier, H., Davis, A. P., Jabin, I., and Bartik, K. (2019). Repositioning Chloride Transmembrane Transporters: Transport of Organic Ion Pairs. *Angew. Chem. Int. Ed.* 58, 6921–6925. doi:10.1002/anie.201900818
- Howe, E. N. W., Busschaert, N., Wu, X., Berry, S. N., Ho, J., Light, M. E., et al. (2016). pH-Regulated Nonelectrogenic Anion Transport by Phenylthiosquaramides. *J. Am. Chem. Soc.* 138, 8301–8308. doi:10.1021/jacs.6b04656
- Kaushik, V., Yakisich, J., Kumar, A., Azad, N., and Iyer, A. (2018). Ionophores: Potential Use as Anticancer Drugs and Chemosensitizers. *Cancers.* 10, 360. doi:10.3390/cancers10100360
- Kevin, D. A., II, Dion, A., Meujo, D. A. F., and Hamann, M. T. (2009). Polyether Ionophores: Broad-Spectrum and Promising Biologically Active Molecules for the Control of Drug-Resistant Bacteria and Parasites. *Expert Opin. Drug Discov.* 4, 109–146. doi:10.1517/17460440802661443
- Li, H., Valkenier, H., Judd, L. W., Brotherhood, P. R., Hussain, S., Cooper, J. A., et al. (2016). Efficient, Non-toxic Anion Transport by Synthetic Carriers in Cells and Epithelia. *Nat. Chem.* 8, 24–32. doi:10.1038/NCHEM.2384
- Lloyd, S. E., Pearce, S. H. S., Fisher, S. E., Steinmeyer, K., Schwappach, B., Scheinman, S. J., et al. (1996). A Common Molecular Basis for Three Inherited Kidney Stone Diseases. *Nature.* 379, 445–449. doi:10.1038/379445a0
- Moore, S. J., Cally, J. E. H., González, J., Sutton, J. L., Brooks, S. J., et al. (2013). Chloride, Carboxylate and Carbonate Transport by Ortho-Phenylenediamine-Based Bisureas. *Chem. Sci.* 4, 103–117. doi:10.1039/c2sc21112b
- Mora, N. L., Bahreman, A., Valkenier, H., Li, H., Sharp, T. H., Sheppard, D. N., et al. (2016). Targeted Anion Transporter Delivery by Coiled-Coil Driven Membrane Fusion. *Chem. Sci.* 7, 1768–1772. doi:10.1039/c5sc04282h
- Oxford Diffraction (2008). *CrysAlis CCD and CrysAlis RED*. Yarnton, United Kingdom: Oxford Diffraction Ltd.
- Peng, C.-C., Zhang, M.-J., Sun, X.-X., Cai, X.-J., Chen, Y., and Chen, W.-H. (2016). Highly Efficient Anion Transport Mediated by 1,3-Bis(benzimidazol-2-yl)benzene Derivatives Bearing Electron-Withdrawing Substituents. *Org. Biomol. Chem.* 14, 8232–8236. doi:10.1039/c6ob01461e
- Picci, G., Kubicki, M., Garau, A., Lippolis, V., Mocci, R., Porcheddu, A., et al. (2020). Simple Squaramide Receptors for Highly Efficient Anion Binding in Aqueous Media and Transmembrane Transport. *Chem. Commun.* 56, 11066–11069. doi:10.1039/D0CC04090H
- Pomorski, R., García-Valverde, M., Quesada, R., and Chmielewski, M. J. (2021). Transmembrane Anion Transport Promoted by Thioamides. *RSC Adv.* 11, 12249–12253. doi:10.1039/D1RA01646F
- Pusch, M. (2007). *Chloride Movements across Cellular Membranes, Advances in Molecular and Cell Biology*. 1st edn., Vol. 38. Amsterdam, Netherlands: Elsevier
- Saha, A., Akhtar, N., Kumar, V., Kumar, S., Srivastava, H. K., Kumar, S., et al. (2019). pH-Regulated Anion Transport Activities of Bis (Iminourea) Derivatives across the Cell and Vesicle Membrane. *Org. Biomol. Chem.* 17, 5779–5788. doi:10.1039/c9ob00650h
- Sheldrick, G. M. (2015a). SHELXT—Integrated Space-Group and Crystal-Structure Determination. *Acta Cryst.* A71, 3–8. doi:10.1107/S2053273114026370
- Sheldrick, G. M. (2015b). Crystal Structure Refinement with SHELXL. *Acta Cryst.* C71, 3–8. doi:10.1107/S2053229614024218
- Sheppard, D. N., Rich, D. P., Ostedgaard, L. S., Gregory, R. J., Smith, A. E., and Welsh, M. J. (1993). Mutations in CFTR Associated with Mild-disease-form Cl<sup>-</sup> Channels with Altered Pore Properties. *Nature.* 362, 160–164. doi:10.1038/362160a0
- Simon, D. B., Bindra, R. S., Mansfield, T. A., Nelson-Williams, C., Mendonca, E., Stone, R., et al. (1997). Mutations in the Chloride Channel Gene, CLCNKB, Cause Bartter's Syndrome Type III. *Nat. Genet.* 17, 171–178. doi:10.1038/ng1097-171
- Simon, D. B., Karet, F. E., Hamdan, J. M., Pietro, A. D., Sanjad, S. A., and Lifton, R. P. (1996). Bartter's Syndrome, Hypokalaemic Alkalosis with Hypercalciuria, Is Caused by Mutations in the Na–K–2Cl Cotransporter NKCC2. *Nat. Genet.* 13, 183–188. doi:10.1038/ng0696-183
- Sperelakis, N., and Sperelakis, N. (2012). *Chapter 4: Ionophores in Planar Lipid Bilayers, Cell Physiology Sourcebook: Essentials of Membrane Biophysics*. 4th edn.. London, UK. 978-0-12-387738-3
- Saha, T., Hossain, M. S., Saha, D., Lahiri, M., and Talukdar, P. (2016). Chloride-Mediated Apoptosis-Inducing Activity of Bis(sulfonamide) Anionophores. *J. Am. Chem. Soc.* 138, 7558–7567. doi:10.1021/jacs.6b01723
- Valkenier, H., Dias, C. M., Goff, K. L. P., Jurček, O., Puttreddy, R., Rissanenb, K., et al. (2015). Sterically Geared Tris-Thioureas; Transmembrane Chloride Transporters with Unusual Activity and Accessibility. *Chem. Commun.* 51, 14235–14238. doi:10.1039/c5cc05737j
- Valkenier, H., Judd, L. W., Li, H., Hussain, S., Sheppard, D. N., and Davis, A. P. (2014). Preorganized Bis-Thioureas as Powerful Anion Carriers: Chloride Transport by Single Molecules in Large Unilamellar Vesicles. *J. Am. Chem. Soc.* 136 (35), 12507–12512. doi:10.1021/ja507551z
- Wang, Z.-K., Hong, X.-Q., Hu, J., Xing, Y.-Y., and Chen, W.-H. (2021). Synthesis and Biological Activity of Squaramido-Tethered Bisbenzimidazoles as Synthetic Anion Transporters. *RSC Adv.* 11, 3972–3980. doi:10.1039/d0ra10189c
- Welsh, M. J., and Smith, A. E. (1993). Molecular Mechanisms of CFTR Chloride Channel Dysfunction in Cystic Fibrosis. *Cell.* 73, 1251–1254. doi:10.1016/0092-8674(93)90353-R
- Weselinski, L. J., Luebke, R., and Eddaoudi, M. (2014). A Convenient Preparation of 9H-Carbazole-3,6-Dicarbonitrile and 9H-Carbazole-3,6-Dicarboxylic Acid. *Synthesis.* 46, 596–599. doi:10.1055/s-0033-1340557
- Yu, X.-H., Peng, C.-C., Sun, X.-X., and Chen, W.-H. (2018). Synthesis, Anionophoric Activity and Apoptosis-Inducing Bioactivity of Benzimidazolyl-Based Transmembrane Anion Transporters. *Eur. J. Med. Chem.* 152, 115–125. doi:10.1016/j.ejmech.2018.04.036
- Zeng, L. Z., Zhang, H., Wang, T., and Li, T. (2020). Enhancing K<sup>+</sup> Transport Activity and Selectivity of Synthetic K<sup>+</sup> Channels via Electron-Donating Effects. *Chem. Commun.* 56, 1211–1214. doi:10.1039/C9CC08396K

**Conflict of Interest:** The authors declare that the research was conducted in the absence of any commercial or financial relationships that could be construed as a potential conflict of interest.

Copyright © 2021 Maslowska-Jarzyna, Korczak and Chmielewski. This is an open-access article distributed under the terms of the Creative Commons Attribution License (CC BY). The use, distribution or reproduction in other forums is permitted, provided the original author(s) and the copyright owner(s) are credited and that the original publication in this journal is cited, in accordance with accepted academic practice. No use, distribution or reproduction is permitted which does not comply with these terms.